*36th EPS Conference on Plasma Phys. Sofia, June 29 - July 3, 2009 ECA Vol.**33E**, P-5.183 (2009)*

Results of reflectometry studies on ELM dynamics in JET

*S. Soldatov[2,3], A. Fonseca[1], Y. Liang[3], J. Fessey[1], A. Sirinelli[1], A. Krämer-Flecken[3], G. Van Oost[2] and JET-EFDA contributors**

JET-EFDA Culham Science Centre, Abingdon, OX14 3DB, UK

[1]EURATOM-UKAEA Fusion Association, Culham Science Centre, Abingdon, UK

[2]Department of Applied Physics, Ghent University, Rozier 44, 9000 Gent Belgium

[3]Institut für Energieforschung-Plasmaphysik, Forschungszentrum Jülich GmbH, Association EURATOM-FZJ, Trilateral Euregio Cluster, D–52425 Jülich, Germany

*See F. Romanelli, Fusion Energy 2008 (Proc. 22nd IAEA Conf., Geneva, 2008) IAEA Vienna

Introduction. The H-mode pedestal and the edge localized mode (ELM) driven by pedestal gradients are two crucial issues remaining in the focus of magnetic fusion research for last twenty years [1]. The effect of transient peak loads on the divertor target plates due to ELM pulses is recognized as one of the most important aspects defining the design of future devices. In spite of big progress in the characterization of the H-mode pedestal [2], the ELM physics remains an open issue up to now. In the view of short time scale of ELM crash only a few diagnostics are able to follow the ELM dynamics. One of them is a reflectometry and some recent works have shown its ability [3, 4]. JET X-mode reflectometer [6] operates at four fixed frequencies (76, 85, 92 and 103 GHz) simultaneously. They are distant sensibly to give cutoff layers covering the pedestal region from top to foot in most H-mode plasmas. Our paper describes the recent results on the study of ELM dynamics with X-mode reflectometer in JET.

Experimental results. The measurement were performed in several H-mode JET plasmas with following parameters: plasma current $I_p \simeq 2\ MA$, toroidal field $B_t = 1.8$ and $2.7\ T$, electron density $n_e(0) \sim 5 \div 8 \cdot 10^{19} m^{-3}$, neutral beam heating $P_{NBI} \sim 12 \div 16\ MW$. For one of such shots, #76001, the spectrograms with the time and frequency resolutions of $\Delta t = 1$ ms and

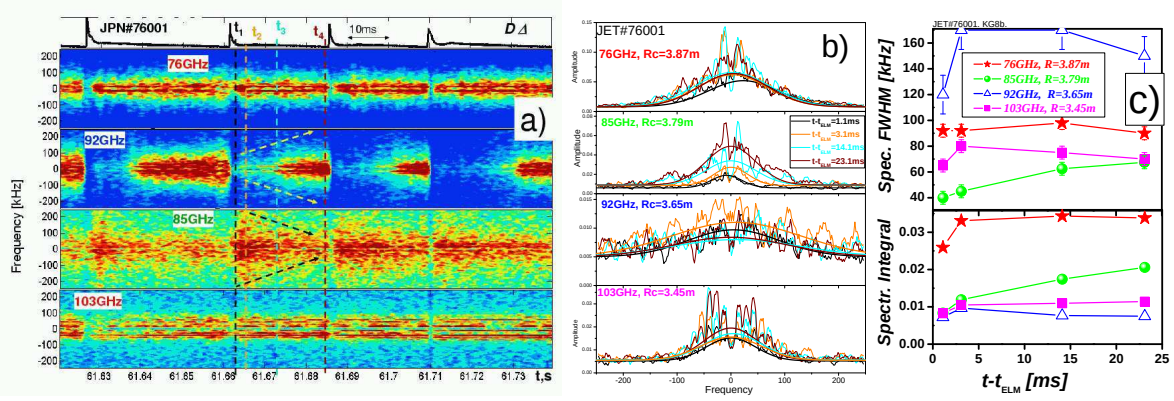

Figure 1: ***(a)** Reflectometer spectrograms. **(b)** Fourier spectra for 4 consequent times between 2nd and 3d ELMs shown on (a). **(c)** FWHM and integral of spectra shown on (b).*

$\Delta f = 1$ kHz accordingly are plotted in Fig.1a. The probing frequencies 76, 85, 92 and 103 GHz correspond to the cutoff positions calculated from LIDAR system: $R \approx 3.87, 3.79, 3.65$ and 3.45 m. The radius of last closed flux surface (LCFS) is R=3.88 m and the pedestal top is at $R \approx 3.78$ m. Thus, 76 GHz channel is reflected 1-2 cm inside LCFS near the pedestal foot; the cutoff layer for 85 GHz channel is inside the pedestal and 92 and 103GHz channels are reflected ≈ 10 and ≈ 30 cm dipper with respect to pedestal top. The D_α signal is shown as a reference on the upper plot where 4 ELM events are seen. All spectrograms are clearly modulated by the ELMs, although the cutoff positions are separated by ≈ 40 cm . Such a deep modulation is usual for H-mode plasmas with moderate densities and was observed with ECE diagnostics at JET earlier. The most significant variations are found to be in the spectrum of 85 GHz channel (R=3.79 m). After the ELM crash its amplitude drops and recovers continuously towards the next ELM, the spectrum broadens during the recovery phase. As opposed to that, the 92 GHz signal shows a different dynamics - it broadens within 4-5 ms after the ELM crash and thereafter shrinks continuously towards the next ELM. The 76 GHz signal having most peripheral reflection reduces in amplitude after the ELM crash only for the short time and recovers quickly within 2-3 ms. Nearly the same behavior is observed for the 103 GHz channel. For the evaluation of dynamics in spectral amplitude and the spectrum full width at half maximum (FWHM) Fourier amplitude spectra are represented on the Fig.1b with $\Delta f = 2$ kHz. These spectra correspond to four different times between 2^{nd} and 3^{d} ELMs shown on the Fig.1a: $t - t_{ELM} = 1.1, 3.1, 14.1, 23.1$ ms. The experimental spectra are fitted by the Gaussian functions to perform the estimation of FWHM taken above the confidence level. The FWHM is plotted on the Fig.1c together with the spectrum integral $I_{sp} = \frac{1}{nfft} \cdot \sum F(\omega_i)$ taken over $2 < \omega/2\pi < 250$ kHz. If the FWHM of the k-spectrum

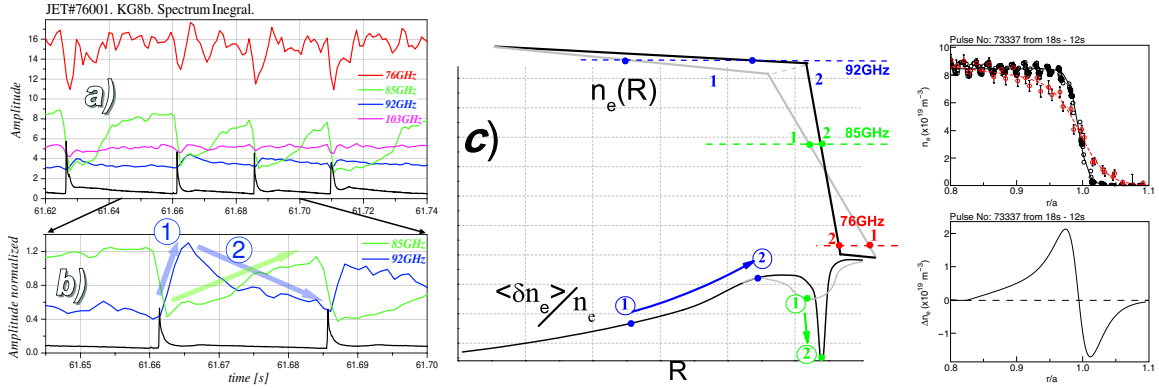

Figure 2: ***(a)*** *Spectrum integral traces for 4 probing frequencies.* ***(b)*** *Different dynamics of "85" and "92" signals (normalized).* ***(c)*** *Model of $n_e(R)$ and $\frac{\delta n_e}{n_e}(R)$ evolution.* ***(d)*** *Experimental example of $n_e(R)$ dynamics [7].*

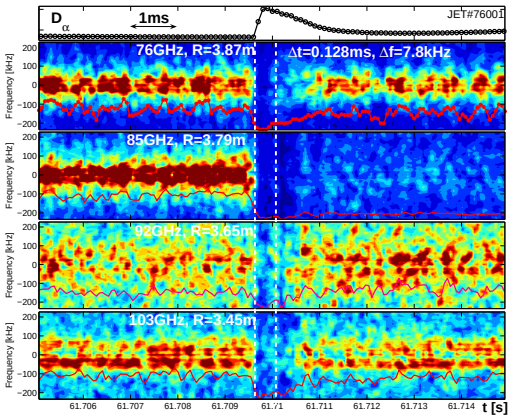

Figure 3: *Spectrograms with* $\Delta 128\mu s$.

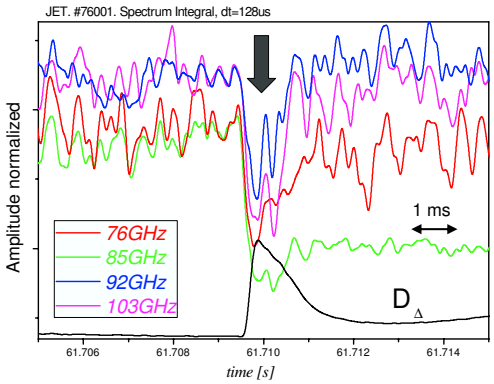

Figure 4: $I_{sp}(t)$ *traces (normalized).*

varies not much then the FWHM of f-spectrum is defined by Doppler Effect, $f = k \cdot \upsilon / 2\pi$, and $I_{sp} = F(\upsilon)$, that agrees with Fig.1c. For 85 GHz the increase in the spectrum width is of the order of 60% that correlates with the increase in $I_{sp,86}$ by 100% within $1 < t - t_{ELM} < 23$ ms. The same is for 92 GHz channel, its spectrum varies non-monotonically by $\approx 30 - 40\%$ along $I_{sp,92}$. The spectra FWHM for 76 GHz and 103 GHz vary only a little. While the fluctuations in reflectometer signals linked with the density fluctuation level $< \tilde{n}/n >$ and local permittivity scale length L_ε as $< \varphi >_{refl} \sim < \tilde{n}/n > \cdot \sqrt{L_\varepsilon}$ [5], the spectrum integral can be expressed as $I_{sp} = F(< \tilde{n}/n >, \sqrt{L_\varepsilon}, \upsilon)$. Now we will consider the dynamics of reflectometer signals from the point of view of the radial and time distribution of $< \tilde{n}/n >$ and L_n. In Fig.2a the spectral dynamics of reflectometer signals is represented in the integral form ($I_{sp} = \frac{1}{nfft} \cdot \sum F(\omega_i)$) with $\Delta t = 1$ ms and on the same time scale as in Fig.1a. More detailed zoom for 85 GHz and 92 GHz channels is presented in Fig.2b for normalized traces. For the explanation of observed dynamics a model considering the evolution of density profile and profile of the density fluctuations at the plasma edge is proposed (see Fig.2c). We assume a strong suppression of the density fluctuations within narrow region near the barrier and monotonically increasing (from center towards edge) turbulence level in the rest of plasma. It is assumed also that $n_e(R)$ profile evolves around pivot point during ELM crash. Such a model is consistent with the recent experimental findings with HRTS [7] (shown in Fig.2 at rhs). The positions of the cutoffs for 76 GHz, 85 GHz and 92 GHz systems are shown on the graph and marked as "1" for the profile after ELM crash and as "2" for the profile before crash. Note that the absolute radial positions here are not of importance, only the relative positions with respect to each other and minimum of $\frac{\delta n_e}{n_e}$(R) are sufficient. In the framework of the model i) the non-monotone dynamics of $I_{sp,92}$ cannot be explained because both $\frac{\delta n_e}{n_e}$ and L_n monotone increases; ii) monotonically increasing dynamics of $I_{sp,85}$ cannot be explained as well while both $\frac{\delta n_e}{n_e}$ and L_n decreases sig-

nificant within the pedestal. iii) The interpretation of 76 GHz channel is most difficult while the profile of $\frac{\delta n_e}{n_e}$ behind the LCFS is less predictable. Nevertheless looking on the experimental example presented in Fig.2d we can suppose that cutoff during recovery stage moves inwards and L_n decreases that again contradicts to observations for 76 GHz channel. A special effort was undertaken trying to resolve the crash stage by a reducing of the analysis resolution time to $\sim 100\mu$s. The results are presented in Figures 3 and 4 with $\Delta t = 0.128$ ms, $\Delta f = 8$ kHz. Note, the DC component of signals is not considered here and we follow only the dynamics of AC component of complex signal within $8 < f < 220$ kHz. One can see that after the ELM crash the amplitude in all channels drops within 100μs to extremely low level. It recovers back within $\sim 200 \div 400\mu$s for channels "76GHz", "92GHz" and "103GHz" whereas the channel "85GHz" (the closest to the pedestal) recovers longer $\sim 1000\mu$s. This indicative drop happens without delay with respect to D_α burst and simultaneously in all four signals (within the time resolution of 128μs). Note, while the "76", "92" and "103" signals recover back quickly this characteristic drop is integrated on the Fig.1, 2.

Conclusions. The model based on the sensible assumptions about the character of turbulence level and density scale length radial distribution and their time evolution during ELM (Fig.2) is unsuccessful to explain the observed dynamics of reflectometry signals. Very probably that there are some other factors evolving on the ELM time scale and defining the reflectometer signals dynamics. One of possible candidates - plasma rotation and the indirect indication of that was found exploring the spectra FWHM (Fig1). Note, the analysis presented here is performed neglecting the DC component of the reflectometry signals that cannot influence the final conclusions stated in the paper. The fast ($\sim 100\mu$s) and global ($\Delta R \sim 40$ cm) phenomenon during ELM crash is observed: simultaneous drop of fluctuations in all reflectometry signals. It can be explained either i)by the fast variation of the rotation profile (e.g. temporal braking) or ii)by the large and fast variations in the density scale length or iii)by the significant temporal turbulence suppression in the region of ~ 40 cm extension. We cannot exclude also the temporal lost of the probing waves due to the deflection because of reflecting surface deformation. The additional studies are certainly needed to clarify the physics is behind.

References

[1] F. Wagner, Plasma Phys. Control. Fusion 49 (2007) B1-B33
[2] A.W. Leonard, Journal of Phys. (Conf. Series) 123 (2008) 012001
[3] N. Oyama, et al, Plasma Phys. Control. Fusion 43 (2001) 717-726
[4] L. Zeng, et al, Plasma Phys. Control. Fusion 46 (2004) A121-A129
[5] E. Mazzucato, Review Sci. Instr. Vol.69, No.6, June 1998, 2201-2217
[6] S. Hacquin et al., Review Sci. Instr. Vol.75, No.10, October 2004, 3834
[7] M.N.A. Beurskens et al., submitted to Nucl. Fusion, 2009